

From stem cells to functional lymphocytes: cell differentiation and gene therapy implementation for RAG-SCID

García Pérez, L.

Citation

García Pérez, L. (2021, October 6). From stem cells to functional lymphocytes: cell differentiation and gene therapy implementation for RAG-SCID. Retrieved from https://hdl.handle.net/1887/3214836

Version: Publisher's Version

Licence agreement concerning inclusion of doctoral

License: thesis in the Institutional Repository of the University

of Leiden

Downloaded from: https://hdl.handle.net/1887/3214836

Note: To cite this publication please use the final published version (if applicable).



ABSTRACT

Recombinase-activating gene 2 (RAG2) deficient SCID patients lack B and T lymphocytes due to the inability to rearrange immunoglobulin and T-cell receptor genes. RAG2, together with RAG1, is required as a dimer to initiate lymphoidspecific V(D)J recombination. Curative treatment for this form of SCID is limited and confined to allogenic hematopoietic stem-cell transplantation; however, gene therapy might be a valid alternative especially for patients lacking a suitable bone marrow donor. We focused on clinically relevant lentivirus SIN vectors (LV) containing different internal promoters (EFS, MND, PGK, UCOE) driving a codon optimized (c.o.) version of the RAG2 (c.o.RAG2) gene to ensure optimal expression at low vector copy numbers (VCN). Lineage-depleted mouse bone marrow cells were transduced with the novel lentiviral SIN vectors and transplanted into Rag2-/mice, which were used as a preclinical model to assess efficacy and safety. Immune reconstitution and functional restoration of RAG2 deficiency was obtained with our MND-, PGK- and UCOE c.o.RAG2 LV. However, the UCOE-c.o.RAG2 LV production appeared to be troublesome, and the MND-c.o.RAG2 LV raised genotoxicity and integration concerns in addition to high RAG2 expression that seems to hamper Bcell development. We conclude that functional restoration of RAG2 deficiency at low VCN can be achieved with clinically acceptable vectors using the PGK as suitable promoter, which allows for sufficient but not detrimentally high RAG2 expression.

INTRODUCTION

Severe combined immunodeficiency (SCID) is a rare life-threatening inhered disorder of the immune system, characterized by the absence of functional T cells due to their developmental arrest in the thymus, often accompanied by deficiency in B cells and/or NK cells ¹⁻³. The lack of a functional adaptive immune response affects infants' failure to thrive. associated with severe and recurrent opportunistic infections and other metabolic abnormalities that are invariably fatal within the first year of life unless effective treatment is provided. SCIDs represent the most severe forms of primary immunodeficiencies and represents a real pediatric emergency. The phenotype of SCID depends on the underlying genetic defect with over 20 different genes being shown to be causative of SCID 4, 5 and persisting cases (around 20%) of affected infants without a known genetic cause ^{3, 6}. One of the main pathways that can be affected by the molecular defect is the V(D)J recombination. V(D)J recombination is a complex process that occurs in early B- and Tcell development leading to a functional Immunoglobulins (Igs) and T-cell receptors (TCRs) respectively. The deficiency in genes involved in the recombination process like RAG1 and RAG2 7 lead to T-B-NK+ form of SCID with an autosomal recessive trait characterized by the absence of functional TCR and Iqs. RAG1 and RAG2 proteins form a heterodimer complex at the beginning of the V(D)J recombination process mediating the binding and cleavage of the DNA. Deficiency of one of these proteins is associated with a limited production of T and B cells, associated with the absence of V(D)J recombination causing cell apoptosis. To date, the principal effective treatment is limited and confined to allogeneic hematopoietic stem cell (HSC) transplantation for most of the deficiencies 8, 9, with emerging autologous HSC gene therapy options ¹⁰⁻¹² including for RAG1 SCID ¹³.

Attempts to develop autologous HSC gene therapy to correct RAG2 deficiency have been made by several groups, aiming to relieve the early block in T- and B-cell differentiation by conferring a selective advantage of the gene corrected cells over the uncorrected cells. In these studies the Rag2 knock-out (Rag2-/-) murine model with severe and early block of both B- (pro B stage) and T- (double negative DN stage) cell development, identical to the human phenotype, was used to verify the gene therapy approaches. Murine HSCs were transduced by gammaretroviral transfer-based vector bearing a native human RAG2 transgene. A sustained correction of the immune deficiency without side effects was observed, demonstrating the efficiency of ex vivo RAG2 gene transfer in HSCs 14. Unfortunately, clonal T-cell proliferation and adverse effects due to transgene insertions near to proto-oncogenes was detected in diverse clinical trials using gammaretroviral vectors ¹⁵⁻¹⁸. RAG2 gene transfer was therefore updated to safer lentiviral vectors (LV) and improved by codon optimization. Codon optimization of RAG2 (c.o.RAG2) lentiviral vector resulted in improved viral production and robust immune reconstitution, driving significant increases in viral titers as well as in B- and T-cell reconstitution. Although immune function was corrected, no safety assessment was reported ¹⁹.

Therefore, we set out to develop a new set of SIN lentiviral vectors to express *c.o.RAG2* with different types of promoters (EFS ²⁰, MND ²¹, PGK ²² and UCOE ²³) and to test their ability and safety to correct Rag2 deficiency in the preclinical RAG2-/- mouse model at low vector copy numbers. This set-up allowed us to directly address the effects of differences

in *RAG2* expression in a gene therapy setting. In addition, it has enabled us to select a new SIN LV vector that functionally corrects the Rag2 deficiency *in vivo* in mice with no adverse effects. The PGK-c.o.RAG2 is our vector of choice capable of providing an appropriate RAG2 expression and therefore a valid gene therapy option for the treatment of RAG2 deficiency and to test their ability and safety to correct Rag2 deficiency in the preclinical RAG2-/- mouse model at low vector copy numbers. This set-up allowed us to directly address the effects of differences in *RAG2* expression in a gene therapy setting. In addition, it has enabled us to select a new SIN LV vector that functionally corrects the Rag2 deficiency *in vivo* in mice with no adverse effects. The PGK-c.o.RAG2 is our vector of choice capable of providing an appropriate RAG2 expression and therefore constituting a valid gene therapy option for the treatment of RAG2 deficiency.

MATERIALS AND METHODS

Mice

Balb/c Rag2/II2rg double-knockout mice were a kind gift from Dr. E.J.Rombouts from the Department of Hematology at Erasmus MC (University Medical Center Rotterdam, The Netherlands) or were purchased from Taconic Biosciences, Inc (C.129S6(B6)-Rag2^{tm1Fwa} N12). Balb/c wild-type mice were purchased from Charles River (France). Mice were bred and maintained in the animal facility of Leiden University Medical Center (LUMC). All animal experiments were approved by the Dutch Central Commission for Animal experimentation (Centrale Commissie Dierproeven, CCD).

Lentiviral vectors and lentiviral production

Optimized RAG2 sequence was synthesized by GenScript USA. Codon optimized RAG2 (c.o.RAG2) was cloned into self-inactivating lentiviral pCCL plasmid harbouring different promoters resulting in pCCL-EFS-c.o.RAG2 (hereafter: EFS-c.o.RAG2; elongation factor 1α short promoter) ²⁰, pCCL-MND-c.o.RAG2 (hereafter: MND-c.o.RAG2; myeloproliferative sarcoma virus enhancer, negative control region deleted, dl587rev primer binding site substituted promoter) ²¹, pCCL-PGK-c.o.RAG2 (hereafter: PGK-c.o.RAG2; human phosphoglycerate kinase-1 promoter) ²² and pCCL-UCOE-c.o.RAG2 (hereafter: UCOE-c.o.RAG2; the modified chromatin-remodeling element, devoid of unwanted splicing activity and minimized read-through activity) ²³. DNA sequencing of the transgene was performed to validate the gene transfer construct. Helper plasmids pMDLg/pRRE, pRSV-Rev and pMD2.VSVG for lentiviral production were kindly provided by L.Naldini (San Raffaele Telethon Institute for Gene Therapy, Milan, Italy) ²². Large-scale helper-plasmids were obtained from Plasmid Factory (Bielefield, Germany).

293T cells were transiently transfected with the transfer and helper plasmids using X-tremeGene HP DNA transfection reagent (Sigma-Aldrich). Lentiviruses were harvested 24h, 30h and 48h after transfection, filtered through 0.45µm pore filters (Whatmann) and stored at -80°C. Pooled lentiviral supernatant was concentrated by ultracentrifugation (Beckman Optima[™] LE-80K, rotor SW32Ti) for 16 hours at 10.000 rpm and 4°C under vacuum conditions. Pellets were resuspended in StemSpan Serum-Free expansion medium (SFEM; Stemcell Technologies Inc) and aliquoted to avoid multiple freeze/thaw

cycles. Since no suitable anti-c.o.RAG2 antibodies are available, we determined the viral titer using qPCR as described later on.

Murine HSPC isolation and transduction

Murine bone marrow (BM) cells were obtained from femurs and tibias of Balb/c wild-type and Balb/c Rag2-/- mice. The obtained bones were crushed, cells were passed through a 0,7 µm cell strainer (Falcon), washed and viable frozen. Depletion of lineage-positive cells was performed using the Direct Lineage Cell Depletion kit from Miltenvi Biotec, to isolate hematopoietic stem cell from frozen murine bone marrow. In short, cells were magnetically labelled with the Direct Lineage Cell Depletion Cocktail and incubated for 10min at 4°C. Lineage negative cells were subsequently enriched using the appropriate magnetic columns and the MACS separator (Miltenvi Biotec). Directly enriched HSPC were stimulated overnight in StemSpan™-SFEM (StemCell Technologies Inc) supplemented with Penicilin/Streptamycin (5000 units/5000ug/mL; Gibco), 50ng/mL recombinant mouse FMS-related tyrosine 3 ligand (rmFlt3L; R&D systems), 100ng/mL recombinant mouse Stem-Cell Factor (rmSCF; R&D systems) and 10ng/mL recombinant mouse thrombopoietin (rmTPO; R&D Systems) at 37°C with 5%CO2. Depletion efficiency and purity of lineage negative population was analysed by flow cytometry with FACSCanto (BD). Rag2-/- cells were subsequently transduced with the different lentiviruses using 4 ug/ml proteamine sulphate (Sigma-Aldrich) and by way of spin-occulation at 800xg and 32°C for 1 hour. Cells were cultured at 37°C, 5% CO₂ for 24h in medium supplemented with cytokines.

Transplantation Rag2-/- mice

Control mock-transduced cells (Balb/c wild-type cells referred as WT control and Rag2-/cells referred as KO control) and transduced Rag2^{-/-} murine cells (equal number of cells per group, up to 2,5*105 cells/mouse depending on the experiment) were mixed with supportive Rag2-/- spleen cells (3*10⁵ cells/mouse) in Iscove's Modified Dulbecco's Medium (IMDM) without phenol red (Gibco) and transplanted by tail vein injection into preconditioned Rag2^{-/-} recipient mice. Recipient mice (8-12 week old mice) were conditioned with a total body single dose irradiation 24h prior the transplantation using orthovoltage Xrays (8.08Gv) or with two consecutive doses of 25 mg/kg Busulfan (Sigma-Aldrich) (48h and 24h prior transplantation). Mice used for transplantation were kept in specified pathogen-free housing. The first four weeks after transplantation mice were fed with additional DietGel recovery food (Clear H2O) and antibiotic water containing 0.07 mg/mL Polymixin B (Bupha Uitgeest), 0.0875 mg/mL Ciprofloxacin (Bayer b.v.) and 0.1 mg/mL Amfotericine B (Bristol-Myers Squibb) and their welfare was monitored daily. Peripheral blood (PB) from the mice was drawn by tail vein puncture every 4 weeks until the end of the experiment. Peripheral Blood, thymus, spleen and bone marrow were obtained from CO2 euthanized mice.

TNP-KLH mice immunization

Mice were immunized with synthetic TNP-KLH antigen 4 weeks before the end of the experiment. 100 μ g TNP-KLH (Biosearch Technologies Inc.) in 50% Imject Alum (Thermo Scientific) was injected intraperitoneal (i.p.). 3 weeks later, mice were boosted i.p. with 100

µg TNP-KLH in PBS. Serum was collected before immunization and 1 week after the boost injection.

Flow cytometry

Single cell suspensions from thymus and spleen were prepared by squeezing the organs through a 70µM cell strainer (BD Falcon) and single cell suspension from bone marrow was made as described above. Erythrocytes in peripheral blood and spleen samples were lysed using NH₄Cl (8,4 g/L)/KHCO₃ (1 g/L) solution (Pharmacy Leiden Academic Hospital). Single cell suspensions were counted on the NucleoCounter 200 or 3000 (Chemometec) and stained with the following anti mouse antibodies from BD Bioscience, eBioscience or BioLegend: CD3e Biotin (145-2C11; AB 394593), CD4 PE-Cy7 (RM4-5; AB 469578), CD8a PerCP (53-6.7; AB 893423), CD11b Biotin (M1/70; AB 312787), CD19 APC (1D3; AB 398483), CD23 Pe-Cy7 (B3B4; AB 469603), CD43 Biotin or PE (S7; AB 2255226 or AB 394609), CD44 APC-Cy7 (IM7; AB 1727481), CD45 FITC (30-F11; AB 394609), CD45R/B220 PerCP or Pe-Cy7 (RA3-6B2; AB 893355 or AB 2341160), CD62L APC (MEL-14; AB 313098), CD93 APC (AA4.1; AB 469466), CD138 PE (281-2; AB 395000), FoxP3 ef450 (FJK-16s; AB 1518812) lgD ef450 (11-26c; AB 1272239), lgM FITC (II/41; AB 394857), TCRb FITC (H57-597; AB 394683), TCRqd PE (GL3; AB 394689) and Sterptavidin APC-Cy7 and ef450 (AB 10054651 and AB 10359739). Briefly, cells were incubated for 30 min at 4°C in the dark with the antibody-mix solution including directly conjugated antibodies at the optimal working solution in FACS buffer (PBS pH 7.4, 0.1% azide, 0.2% BSA). After washing with FACS buffer, a second 30 min incubation step at 4°C was performed with the streptavidin-conjugated antibody solution. When necessary, 7AAD (BD Biosciences) was used as viability dye. Cells were measured on FACS-Cantoll and LSR Fortessa X-20 (BD Biosciences) and the data was analysed using FlowJO software (Tree Star).

Serum immunoglobulin quantification

Murine IgG, IgM, IgE, TNP-specific IgG were determined by a sandwich enzyme-linked immunosorbent assay (ELISA). NUNC Maxisop plates (Thermo Scientific) were coated with unlabeled anti-mouse IgG, IgM (11E10), IgE antibodies (SouthernBiotech). For detection of TNP-specific IgG, plates were coated with synthetic TNP-KLH (Biosearch Technologies Inc.). Blocking was done with 1% BSA/PBS (mouse) for 1h at room temperature (RT) and subsequently serial dilutions of the obtained sera were incubated for 3h at RT. After washing, plates were incubated with biotin-conjugated anti-mouse IgG, IgM, IgE (SouthernBiotec) for 30 min at RT. For detection, plates were incubated for 30 min at RT with streptavidin horseradish peroxidase (Jackson Immuno Research laboratories) and subsequently azino-bis-ethylbenzthiazoline sulfonic acid (ABTS, Sigma-Aldrich) was used as a substrate. Data was acquired at a wavelength of 415 nm using Bio-Rad iMark microplate reader and MPM 6 software (Bio-Rad). Antibody concentration was calculated by using serial dilutions of purified IgG, IgM, IgE proteins (SouthernBiotech) as standards.

Determination vector copy number (VCN) and c.o.RAG2 expression by RT-qPCR

qPCR was used for the quantitative analysis of genomic lentiviral RNA, proviral DNA copies and transgene mRNA expression using WPRE, c.o.RAG2, ABL1 and PTBP2 as

targets (**Table S1**). Total RNA from single cell suspensions was isolated using RNeasy Mini kit (Qiagen) and reverse transcribed into cDNA using Superscript III kit (Invitrogen). Genomic DNA was extracted from single cell suspensions using the GeneElute Mammalian Genomic DNA kit (Sigma-Aldrich). VCN was determined on DNA samples by the detection of WPRE and PTBP2. The levels of transgene expression were determined on cDNA samples, by normalizing *c.o.RAG2* to the expression of the *ABL1* gene. qPCR was performed using TaqMan Universal Master Mix II (Thermofisher) in combination with specific probes for indicated genes from Universal Probe Library (Roche). Primers and probes used are listed in **Table S1**. PCR reactions were performed on the StepOnePlus Real-Time PCR system (Thermofisher). All samples were run in triplicate.

Repertoire analysis

Total RNA was purified from murine spleen cells and reverse transcribed into cDNA as described previously. GeneScan analysis procedure of the murine T-cell repertoire was adapted from ²⁴. cDNA was amplified using a FAM-labeled C gene segment-specific primer along with 24 TCR Vβ-specific primers (See **Table S2**). GeneScanTM 500 ROXTM (ThermoFisher) was used as internal size standard. Labelled PCR products were run on the ABI Prism® Genetic Analyzer (Applied Biosystems) for fragment analysis. Raw spectratype data was analyzed, visualized and scored by ImSpectR, a novel spectratype analysis algorithm for estimating immunodiversity ²⁵. ImSpectR identifies and scores individual spectratype peak patterns for overall (Gaussian) peak distribution; shape of individual peaks, while correcting for out-of-frame TCR transcripts. Scores range from 0 when no peaks detected, to 100 for a diverse TCR repertoire.

In Vitro Immortalization assay (IVIM)

Genotoxic potential of the viral vectors (MND-c.o.RAG2 and PGK-c.o.RAG2) was quantified as previously described by Baum et al. ^{26, 27}.

<u>Insertion site analysis S-EPTS/LM-PCR (shearing extension primer tag selection ligation-mediated PCR)</u>

Lentiviral insertion site was analysed by non-restrictive Linear Amplification Mediated PCR (nrLAM-PCR) on murine BM DNA samples from MND-c.o.RAG2 and PGK-c.o.RAG2 gene therapy mice as described by Schmidt M. et al ²⁸.

S-EPTS/LM-PCR was used to analyse insertion sites and cancer-related gene insertions on murine bone marrow, spleen and thymus DNA samples from PGK-c.o.RAG2 gene therapy mice 24 weeks after transplantation ²⁹⁻³².

RESULTS

Clinically relevant LV suitable to overcome immune RAG2 deficiency

Various clinically relevant self-inactivating (SIN) lentiviral (LV) pCCL plasmids harbouring a codon optimized version of RAG2 (c.o.RAG2) driven by four different promoters were tested in murine Rag2^{-/-} model: EFS-c.o.RAG2 (Elongation factor 1α short promoter) ²⁰, MND-c.o.RAG2 (myeloproliferative sarcoma virus enhancer, negative control region deleted, dl587rev primer binding site substituted promoter) ²¹, PGK-c.o.RAG2 (human

phosphoglycerate kinase-1 promoter) ²² and UCOE-c.o.RAG2 (the modified chromatin-remodelling element, devoid of unwanted splicing activity and minimized read-through activity) ²³ (**Fig 1A**).

Rag2-/- mice were transplanted with wild-type stem cells (WT control), mock transduced Rag2-deficient stem cells (KO Control) or gene therapy treated stem cells using the mentioned four different plasmids (EFS VCN=0.4, MND VCN=0.4, PGK VCN=0.3 and UCOE VCN=0.2). Unfortunately, mice transplanted with stem cells transduced with the EFS-c.o.RAG2 plasmid did not survive the length of the experiment (Fig 1B), and no immune reconstitution was observed compared to the mice transplanted with cells transduced with the other constructs (Fig.S1A). Twenty weeks after transplantation, mice were sacrificed and immune organs were analysed for immune cell reconstitution. B-cell development in the bone marrow of mice transplanted with the remaining constructs was rescued similarly to WT control mice, alleviating the block in the pre-B cell stage in the KO control group, and developing further into immature and mature B cells (Fig. 1C and Fig S1B). Mature B cells were detected in the periphery, blood and spleen, in mice transplanted with the gene therapy cells, albeit in more moderate amounts than WT group (Fig 1D). Similarly, T-cell development was recovered at different extend with the different transplanted gene therapy cells, developing beyond the initial KO block at the double negative (DN; CD4-CD8-) stage (Fig 1E and Fig S1C). Thymocytes in gene therapytreated mice developed into the immature single positive (ISP; CD8+CD3-), double positive (DP; CD4+CD8+) and single positive (SP; CD3+CD4+ or CD3+CD8+) stages within the thymus. Mature CD4 and CD8 T cells successful migrate to the periphery, detecting equal or even higher numbers of T cells than WT control group (Fig 1F). Nicely, all immature and mature B-cell subsets (transitional B cells, marginal zone B cells, memory B cells) as well as CD4 and CD8 T-cell subsets (naïve, effector memory, central memory subsets) were detectable in comparable proportions to WT control mice with the three different constructs (Fig S1D and Fig S1E).

In addition, RAG2 functionality was restored, with successful V(D)J recombination in B cells after gene therapy. Both IgG and IgM were detected in the serum of all gene therapy mice, with significantly increased levels for PGK-c.o.RAG2 and UCOE-c.o.RAG2 compared to the KO serum (**Fig 1G**). Therefore, although gene therapy mice were lagging behind with regard to B-cell numbers, their functionality in the form of antibody production was restored to WT IgM levels. Genescan analysis of up to 24 different T cell receptor Vb genes also revealed the restoration of T-cell receptor rearrangement. The cumulative complexity score of the V β repertoire calculated by ImSpectR 25 showed an active V(D)J recombination machinery able to successfully rearrange TCR genes and provide a diverse TCR Vb repertoire after gene therapy (**Fig 1H**). Overall, gene therapy to treat RAG2 deficiency seems feasible with some of the tested clinically relevant SIN LV such pCCl c.o.RAG2 carrying the MND, PGK or UCOE promoters.

LV production and safety concerns for specific c.o.RAG2

The different lentiviruses were produced by transient transfection of the transfer vectors, GAG-pol, REV and VSV-G plasmids into 293T cells ^{22, 33}. Virus production and expression

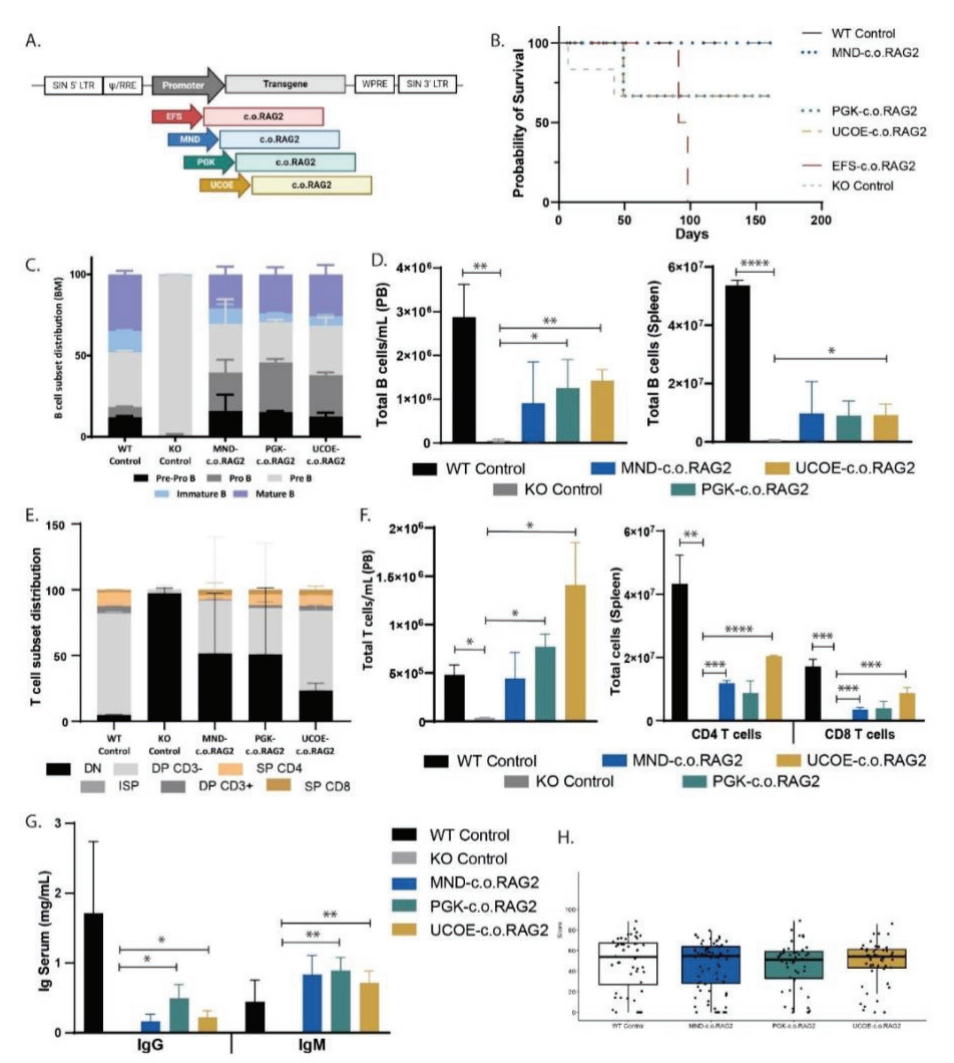


Figure 1: Relevant clinically applicable lentiviral vectors drive immune reconstitution in Rag2-/- mice. A) Four different SIN LV plasmids in the CCL backbone carrying different promoters (EFS, MND, PGK and UCOE promoter) were tested driving the expression of a codon optimized version of RAG2. Rag2 deficient mice (experiment with total 3 mice/group) were transplanted with 100.000-200.000 stem cells: WT cells, mock Rag2 KO cells, EFS-c.o.RAG2 treated KO cells (VCN=0.4), MND-c.o.RAG2 treated KO cells (VCN=0,4), PGK-c.o.RAG2 treated KO cells (VCN=0,3) or UCOE-c.o.RAG2 treated KO cells (VCN=0,2). B) Survival analysis of the different groups of mice: WT control transplanted mice, KO control transplanted mice and EFS-c.o.RAG2, MND-co.o.RAG2 , PGK-c.o.RAG2, UCOE-c.o.RAG2 gene therapy mice. C) Proportion of the different B-cell developmental subsets in the BM. D) Total number of B cells (B220hi+) in the PB (left panel) and spleen (right panel) 20 weeks after SC transplantation. Graphs represent the means and standard deviation of a pilot experiment with 2-3 mice per group. (Multiple t-test, two-tailed, *p≤0,05, **p≤0,01). E) Proportion of the different T-cell developmental subsets in the thymus. F) Total number of T cells (CD3+TCRαβ+) in PB (left panel) and in the spleen (right panel) 20 weeks after transplantation. Graphs represent the means and standard deviation of a pilot experiment with 2-3 mice per group. (Multiple t-test, two-tailed, *p≤0,05, **ap≤0,01).

tailed, *p \leq 0,05, ** $p\leq$ 0,01, *** $p\leq$ 0,001) (DN=Double Negative, ISP=Immature Single Positive, DP=Double Positive, SP=Single Positive cells). G) Quantification of total IgG and IgM in mice serum by ELISA. (Multiple t-test *p<0,05, **p<0.01.) H) TCR V β repertoire analysis by GeneScan. A total of 24 V β families was analysed on spleen cells from 3 mice per group. Overall score of all the families was calculated for the different constructs using ImSpectR ²⁵. (Mann-Whitney test; p values represented on the plot; NS = not significant).

efficiency were evaluated for the different lentiviral vectors produced at small and large scale. Only the vectors showing immune efficacy in vivo previously described (MNDc.o.RAG2, PGK-c.o.RAG2 and UCOE-c.o.RAG2) were produced at large scale. The number of viral particles and infectious genomes of the small and large concentrated batches was assessed by qPCR. Consistently, both the small and large batches of UCOEc.o.RAG2 lentivirus had a significantly lower number of infectious genomes per mL compared to the other MND and PGK vectors (Fig 2A), highlighting a difficulty to scale up its production. Their promoter strength and their ability to correct the Rag2-/- murine model was determined using transduced lineage negative bone marrow cells from Rag2-/- mice. EFS and PGK-c.o.RAG2 were the vectors with lowest promoter strength while MNDc.o.RAG2 is by far the vector leading to higher c.o.RAG2 expression under relevant conditions for in vivo applications (Fig 2B). This high expression driven by the MND promoter was also detected in the BM of gene therapy transplanted mice; high c.o.RAG2 expression was obtained in BM of MND-c.o.RAG2 transplanted mice (transplanted cells VCN=0.4) but not with PGK-c.o.RAG2 (transplanted cells VCN=0.3) or UCOE-c.o.RAG2 (transplanted cells VCN=0.2), which reached expression levels within the native RAG2 expression in BM (native RAG2 expression relative to ABL1 calculated from Immgen.com; marked as a grey bar). Importantly, where high c.o.RAG2 was achieved, the number of mature B cell in the BM of these mice was reduced, indicating a potential detrimental effect of high RAG2 expression in B cell maturation (Fig 2C, left panel). In contrast, c.o.RAG2 expression in the thymus remained overall lower than in BM and within the range of native RAG2 in the specific organ, allowing for the development of a proper DP population (Fig. 2C, central panel). Notably, the promoter strength of the MND-c.o.RAG2 vector in the BM was significantly higher than in spleen or thymus, in accordance with the expression and the B cell development observed in these mice (Fig 2C, right panel). In contrast, the PGK and UCOE promoter showed comparable promoter strength across the immune organs analysed.

As safety is an important aspect for clinical use of gene therapy vectors, the remaining candidates for clinical application, MND-c.o.RAG2 and PGK- c.o.RAG2, lentivirus batches were tested in the *in vitro* immortalization (IVIM) assay, which is the currently accepted (FDA and EMA approved) standard assay for safety of viral vectors. VCN per cell higher than 2 were achieved in this assay with the test vectors (MND and PGK). In three independent IVIM assays, no cytotoxicity was observed of the PGK vector supernatants on lineage negative mouse bone marrow cells, compared to classical RSF91 gamma-retroviral vectors with known mutagenic potential. The frequency of insertional mutagenic events was comparable to mock transduced cells instead suggesting a relatively low risk to elicit insertional transformation in hematopoietic stem and progenitor cells. However,

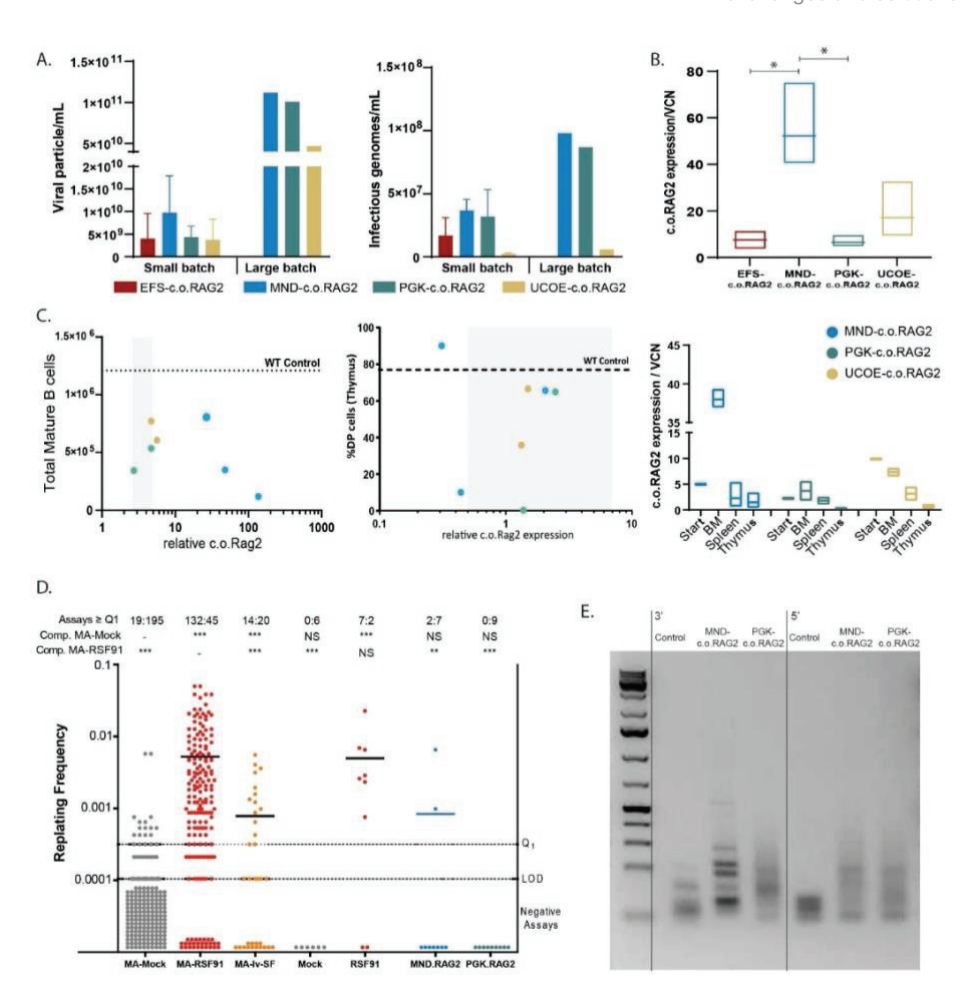


Figure 2: Lentiviral production and safety evaluation of different vectors. A) Production of lentivirus batches in small (two independent batches) and large (one batch) scale with the different constructs. Determination of the number of viral particles (left panel) and of infectious genomes (right panel) per mL after concentration of the lentiviral batches. B) Determination of the promoter strength (c.o.RAG2 expression / VCN) of the different plasmids. Three independent lentivirus batches per plasmid were produced and analysed (One-way ANOVA test *p<0.05: **p<0.01). C) Total number of mature B cells in the BM (left panel) and total percentage of double positive cells in the thymus (middle panel) correlation with the expression of c.o.RAG2 in BM and thymus respectively. (• MND, • PGK, • UCOE promoters, grey window = native RAG2 expression calculated from Immgen). Data shown represents 1 pilot in vivo experiments. Each dot represents one mouse. Non-parametric Spearman r correlation, non-significant). Determination of the promoter strength (c.o.RAG2 expression / VCN) of the different plasmids at the start of the experiment and in the different immune organs of transplanted MND-c.o.RAG2, PGK-c.o.RAG2 and UCOE-c.o.RAG2 mice. D) Data shows results from 3 complete IVIM assays. Replating Frequencies (RF) of the control samples Mock or RSF91 and the test vectors MND-c.o.RAG2 and PGK-c.o.RAG2, in comparison to data of a meta-analysis for control samples (Mock-MA, RSF91-MA, Iv-SF-MA [a lentiviral vector with SFFV promoter]). The data points below the limit of detection (LOD; plates with no wells above the MTT-threshold) were manually inserted into the graph (due to the logarithmic scale of the y-axis). Above the graph, the ratio of positive (left

number) and negative plates (right number) according to the MTT-assay are shown. Differences in the incidence of positive and negative assays relative to Mock-MA or RSF91-MA were analysed by Fisher's exact test with Benjamini-Hochberg correction (*P < 0.05; **P < 0.01; ***P < 0.001; NS = not significant). If above LOD, bars indicate mean RF. E) LV insertion site analysis by nrLAM-PCR of isolated DNA from BM obtained from Rag2-/- untransduced control mouse (Mock), MND-c.o.RAG2 and PGK-c.o.RAG2 gene therapy mice. Gels shows results of the linear amplification from the 3'LTR and 5'LTR respectively (L=1kb plus marker).

mutagenic potential was detected for the MND-c.o.RAG2, with some clones getting immortalized (**Fig 2D**). In agreement, insertion site analysis by rLAM-PCR of BM samples from gene therapy transplanted mice showed an oligoclonal insertion pattern for MND-c.o.RAG2 vector with discrete insertion bands and therefore preferential insertion sites, while PGK-c.o.RAG2 presented a more polyclonal insertion pattern.

Knowing the importance of a precise RAG2 expression level for successful B cell development, our MND-c.o.RAG2 vector leads to RAG2 expression that is too high as well as insertion site safety concerns. Altogether, and taking the challenging production of UCOE-c.o.RAG2 vector into account, we choose our PGK-c.o.RAG2 as a potential LV candidate to correct RAG2 deficiency.

PGK-c.o.RAG2 LV as potential candidate to correct RAG2 deficiency

Our PGK-c.o.RAG2 vector showed overall satisfactory lentiviral production, correct RAG2 expression levels, safe insertion site profiles and successful immune reconstitution. Therefore, an extensive analysis of ten transplanted gene therapy mice with HSC transduced with the PGK-c.o.RAG2 cells (VCN=0,55) was performed. B-cell development was rescued in BM after gene therapy, overcoming the Rag2-/- block at the pro/pre-B stage and developing into high B220 expressing population with IqD and IqM expressing cells (Fig 3A). The number of B cells in the periphery was recovered, with the total B cells in spleen reaching similar numbers to WT transplanted mice, and significantly different to KO mice (Fig 3B, left graph and Fig S2B). All immature B cell subsets, transitional T1 (IgM^{hi}CD23⁻), T2 (IgM^{hi} CD23⁺) and T3 (IgM^{low} CD23⁺) cells, and mature B cell subsets MB (IgM^{dim/-} CD23⁺) and MZ (IgM⁺CD23⁻), were present after gene therapy (Fig 3B, center and right) in normal proportions. Likewise, the thymocyte developmental block at immature stages was surpassed, although an incomplete block at the DN stage persisted after gene therapy (Fig 3C and Fig S2B). Mature CD4 and CD8 T cells developed and detected in spleen after gene therapy, as seen after transplantation of WT cells. Different subsets of T cells such as naïve, effector memory and central memory T cells were detected in the spleen, to the same extent as in the WT control group (Fig 3D). Importantly, both Tyδ cells (Fig 3E) and FoxP3 CD4 regulatory T cells (Fig 3F) also were restored after gene therapy with PGK-c.o.RAG2 reaching normal WT levels in spleen. T- and B-cell functionality were also restored by PGK-c.o.RAG2 gene therapy. V(D)J recombination in the thymus was achieved allowing a T-cell receptor rearrangement and diversity score as high as in the WT control (Fig 4A). Similarly, IgG and IgM were detected in the serum of the gene therapy mice as well as in WT transplanted mice, indicating successful V(D)J recombination in the BM (Fig 4B).

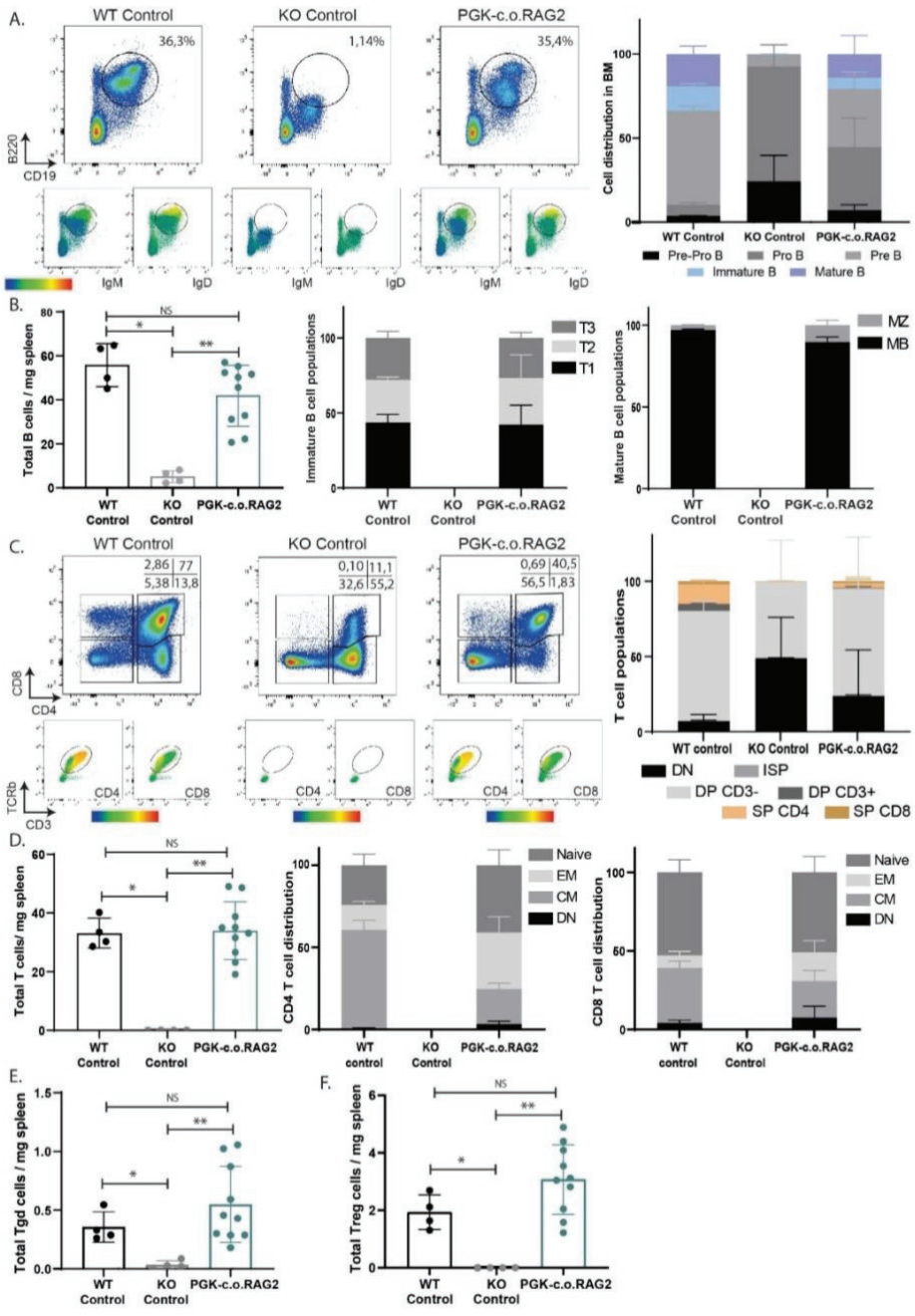


Figure 3: Immune cell reconstitution after gene therapy with the PGK-c.o.RAG2 vector. Rag2 deficient mice were transplanted with 200.000 stem cells: WT cells (4 mice), mock KO cells (4 mice) and PGK-c.o.RAG2 treated cells (VCN=0,55; 10 mice). A. Representative FACS plots showing the restoration of expressing IgD and IgM B220^{hi+} B cells in the BM. Graph representing the proportion of the different B-cell developmental subsets in the BM. B. Total number of B cells (B220^{hi+}) in the spleen

24 weeks after SC transplantation (left panel). Graphs represent the means and standard deviation (Mann-Whitney test, two-tailed, *p \leq 0,05, **p \leq 0,01, NS=non-significant). Immature (B220*CD93* cells; middle panel) and mature (B220*CD93* cells; right panel) B-cell subsets distribution in spleen. (Two-way ANOVA test). C. Representative plots of T-cell development in the thymus (CD4 vs CD8 cells) and T-cell reconstitution in peripheral blood (CD3*TCRab* cells) 24 weeks after transplantation. Graph represents the proportion of the different T-cell developmental subsets in the thymus. (DN=Double Negative, ISP=Immature Single Positive, DP=Double Positive, SP=Single Positive cells). D. Total number of T cells (CD3+TCRa β +) in the spleen (left panel) 42 weeks after transplantation. Graphs represent the means and standard deviation (Mann-Whitney test, two-tailed, *p \leq 0,05, **p \leq 0,01, NS=non-significant). CD4 (middle panel)and CD8 (right panel) T cell subset distribution in the spleen (naïve, effector memory, central memory cells) (Two-way ANOVA test; *p \leq 0,05, **p \leq 0,01, ***p \leq 0,01). E. Total number of Tgd cells in spleen 24 weeks after transplantation (Mann-Whitney test, two-tailed, *p \leq 0,05, **p \leq 0,01, NS=non-significant). F. Total number of Tregs cells in spleen 24 weeks after transplantation (Mann-Whitney test, two-tailed, *p \leq 0,05, **p \leq 0,01, NS=non-significant).

Importantly, IgE was only detected in low amounts (Fig S2B) showing proper functioning of the recombination machinery without causing Omen Syndrome-like features. We used TNP-KLH as T-cell specific antigen and measured the production of TNP specific IgG antibodies, thereby investigating whether the developed T and B cell could collaborate in an active immune response. The TNP-specific IgG level was detected in both mice treated with WT stem cells and gene therapy cells (Fig 4C), showing the potential of a robust immune response after PGK-c.o.RAG2 gene therapy. Considering the importance of c.o.RAG2 expression levels in the BM and the thymus after gene therapy for proper immune cell development, this was analyzed in all animals. Most PGK-c.o.RAG2 gene therapy mice clustered within the native RAG2 expression range in BM and thymus (Fig 4D). Furthermore, insertion site analysis by S-EPTS/LM-PCR on BM, spleen and thymus revealed that all gene therapy mice grouped together within the polyclonal and oligoclonal landscape showing a predominantly polyclonal integration profile composed of low frequency integration events, except for one mouse (Fig 4E). Overall, no particular targeting of cancer genes could be identified.

DISCUSSION

Successful immune B- and T-cell reconstitution and functional V(D)J recombination was achieved after transplantation of HSCs transduced with various clinically relevant lentiviral vectors conferring c.o.RAG2 expression in the Rag2-/- murine model. Although the number of immune cells remained lower than after transplantation with WT HSCs, the recombination machinery function was corrected to WT levels. Various potential applicable promoters led to successful correction of RAG2 deficiency, including the UCOE promoter in accordance with previously data described by Van Til et al. (2012) ¹⁹. However, lentiviral production using the UCOE-c.o.RAG2 plasmid seems to be severely diminished compared to the other tested plasmids, yielding significantly lower infectious genomes in the produced virus supernatant. Although indeed the UCOE-c.o.RAG2 lentiviral vector is a valid option to correct the block in B- and T-cell development due to RAG2 deficiency,

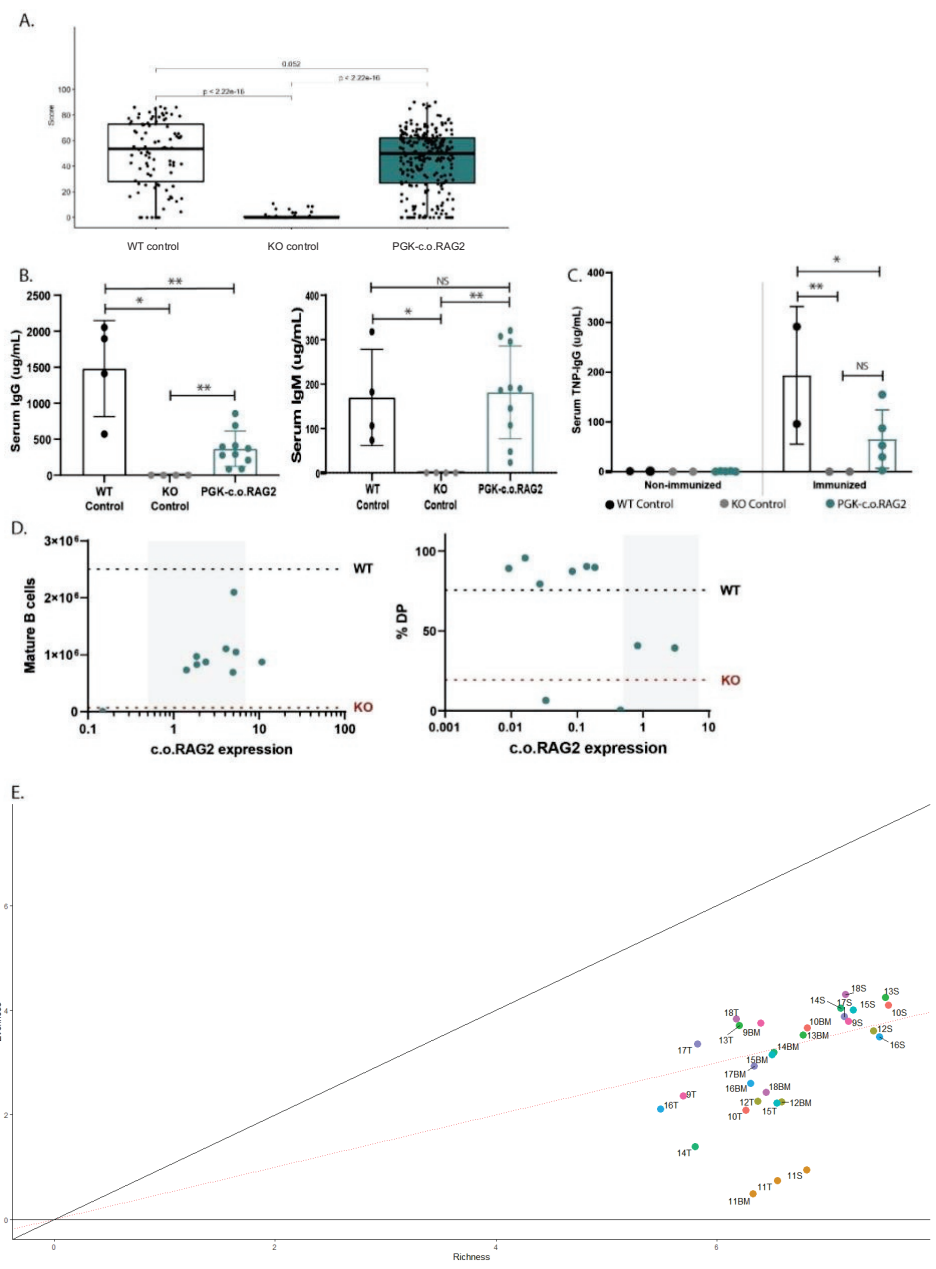


Figure 4: Functional restoration of the immune system after gene therapy with the PGK-c.o.RAG2 vector. A) TCR V β repertoire analysis by GeneScan. A total of 24 V β families was analysed on spleen cells from all mice (4 WT control, 4 KO control and 10 gene therapy mice). Overall score of all the families was calculated for the different constructs using ImSpectR. (Mann-Whitney test; p values represented on the plot). B) Quantification of total IgG and IgM in serum by ELISA (4 mice/control group, 10 PGK-c.o.RAG2 mice) (Mann-Whitney test *p<0,05, **p<0,01, NS=non-

significant) C) Quantification of TNP-specific IgG in serum of non-immunized and immunized mice. Each dot represents a value obtained in one mouse. (4 mice/control group, 10 PGK-c.o.RAG2 mice) (Two-way ANOVA test *p<0,05, **p<0,01, NS=non-significant). D) Total number of mature B cells in the BM (left panel) and total percentage of double positive cells in the thymus (right panel) correlation with the expression of c.o.RAG2 in BM and thymus respectively. Each dot represents one mouse. (Non-parametric Spearman r correlation, non-significant). E) Lentiviral insertion site was analysed by S-EPTS/LM-PCR on murine bone marrow, spleen and thymus DNA samples from 10 PGK-c.o.RAG2 gene therapy mice 24 weeks after transplantation. The samples are placed within the clonal plane regarding richness and evenness of the diversity in the sample. Samples below the red dotted line are considered to be in the mono/oligoclonal area and samples above the red dotted line are in the polyclonal area.

other lentiviral vectors share the same potential and importantly, capable of more efficient viral production which is beneficial for prospective clinical implementation.

A range of c.o.RAG2 expression was detected in vitro and in vivo, depending on the promoter used, with MND carrying the highest promoter strength while other promoter strength remained modest. Interestingly, the highest strength with the MND-c.o.RAG2 vector was specially detected in BM where high c.o.RAG2 expression is driven selectively by this promoter and led to a detrimental effect on mature B-cell numbers unlike previous observations described for the counterpart RAG1 13, 34. Indeed, higher c.o.RAG1 expression in both BM and thymus led to higher and better immune B and T cells reconstitution respectively, only consistently achieved by the strong MND promoter. While this observation was also true for RAG2 gene therapy reconstituted thymi with an improved active DP population at higher c.o.RAG2 expression levels, the overall c.o.RAG2 expression in immune organs was lower than the c.o.RAG1 expression needed for successful immune reconstitution by HSC-based gene therapy in murine models. The different c.o.RAG1 and c.o.RAG2 expression level requirement in immune organs is in accordance with the measured levels of native RAG1 and RAG2 expressions in the mentioned organs, with a higher requirement of RAG1 than RAG2 through the different B and T developmental stages ³⁵.

The undesired effect observed within B cells due to high c.o.RAG2 expression highlighted the importance of the need of a tight RAG2 regulation, especially within the BM where the window of native RAG2 expression is narrow. The exact mechanism underlying this feature need to be further investigated in this *in vivo* model. In accordance with the research from Zheng X. & Schwarz K. (2006) ³⁶ *in vitro*, an excess of RAG2 may inhibit the V(D)J recombination efficiency due to the dysregulation of the phosphorylation and degradation process inherent to the RAG2 protein, which is essential to regulate RAG1/2 activity within the G1 phase. Dysregulation of this process may lead to V(D)J recombination activity within the other cell cycle phases (S/G2/M) where DNA double-strand breaks created by the RAG1/2 complex may be detrimental for cell survival, explaining the lower number of total mature B cells in the BM of mice expressing high c.o.RAG2 in that organ. Further analysis of the cell survival and V(D)J recombination efficiency with our clinically relevant vectors *in vitro* and *in vivo* might help elucidate the importance of tight RAG2 expression.

Furthermore, the MND-c.o.RAG2 vector raises mutagenic and distinct oligoclonal insertion safety concerns resulting in a high toxicity risk. Further insertion site retrieval of the vector *in vivo* and study of the preferential landing sites will reveal if there might be preferential insertion sited located in the vicinity of the transcriptional start site of cancer related genes. Of note, the MND-c.o.RAG2 vector shows clonal expansion capabilities, while the MND vector driving c.o.RAG1 performed as a safer vector ¹³. Therefore, although retrieved data from the IVIM assay was thought to be vector backbone and promoter driven, IVIM results can additionally be a readout of transgene genotoxicity potential.

The clinically relevant PGK-c.o.RAG2, with modest c.o.RAG2 expression within the native RAG2 range in immune organs, emerges as a potential vector for clinical implementation of HSC-based gene therapy to correct RAG2 deficiency. Successful immune reconstitution, with the presence of all different B and T cell subsets, was achieved at acceptable vector copies per cell (VCN=0,55). Functional restoration of the TCR and Ig rearrangements as well as functional T-B cell cooperation was obtained after transplantation, supporting a strong immune response against antigens (TNP-KLH). Phenotypic and functional correction might further improve in the clinical setting, as RAG2 interaction with human RAG1 instead of the murine version might be stronger. In addition, this vector exhibits a safe genotoxicity profile and an oligoclonal/polyclonal skewed safe insertion landscape, without particular targeting of cancer related genes. Gene therapy to correct RAG2 deficiency by gene addition with our PGK-c.o.RAG2 provides a suitable approach; however, clinical implementation can remain challenging due to the tight regulation of RAG2 expression. A more suitable approach to treat RAG2 deficiency, would be gene editing in order to achieve native regulation of RAG2 expression in immune organs.

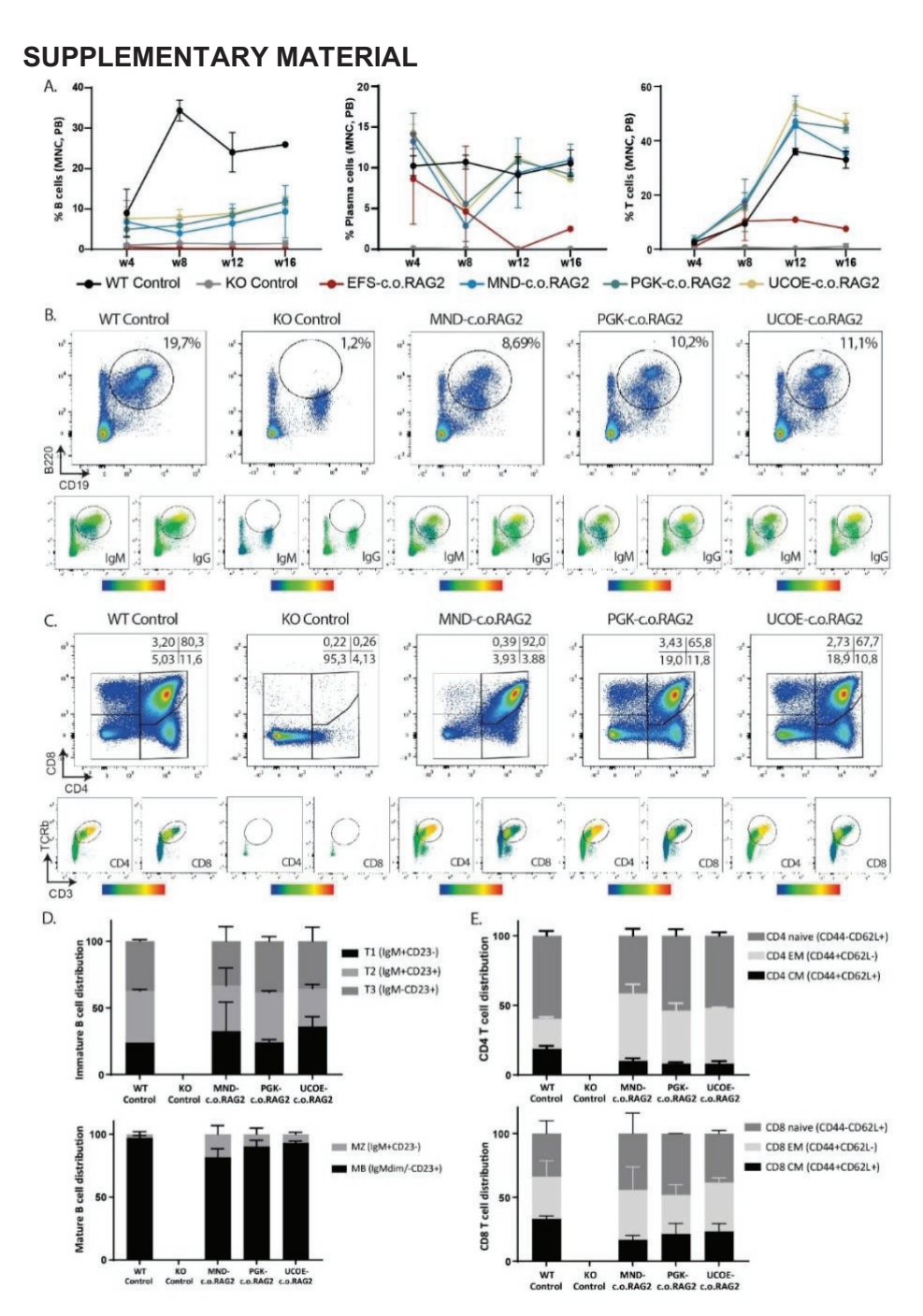


Figure S1: A) Percentage of B cells (CD11b/CD43-B220+ cells; left panel), plasma cells (B220+CD138+; middle panel) and T cells (CD3+TCR $\alpha\beta$ + cells; right panel) over time in PB after stem cell transplantation with the different constructs. B) Representative FACS plots showing the

restoration of expressing IgD and IgM B220hi+ B cells in the BM after gene therapy with 3 different constructs. C) Representative plots of T-cell development in the thymus (CD4 vs CD8 cells) and T-cell reconstitution in the blood (CD3+TCRab+ cells) 24 weeks after transplantation with different gene therapy constructs. D) Immature (B220+CD93+ cells; upper panel) and mature (B220+CD93- cells; lower panel) B-cell subsets distribution in spleen. E) CD4 (upper panel) and CD8 (lower panel) T cell subset distribution in the spleen (naïve, effector memory, central memory cells)

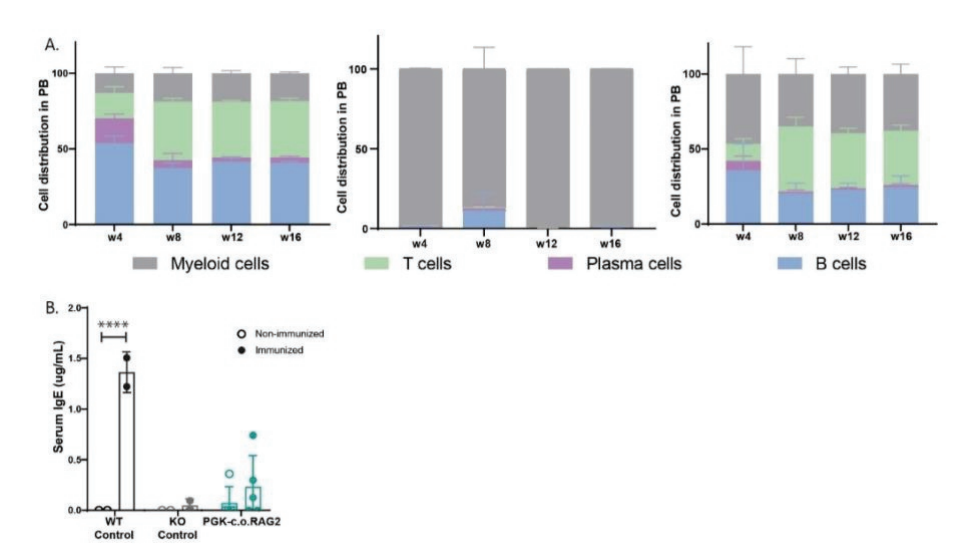


Figure S2: A) Distribution of B cells (CD11b/CD43-B220+ cells), plasma cells (B220+CD138), myeloid cells (CD11b+CD43+) and T cells (CD3+TCRαβ+ cells) over time in PB after stem cell transplantation in WT control, KO control and PGK=c.o.RAG2 transplanted mice. B) Quantification of total IgE in serum by ELISA. Each dot represents a value obtained in one mouse, immunized and non-immunized mice. Two-way Annova test (two tailed, *p<0,05; ****p<0,0001)

Table S1: Determination VCN and c.o.RAG2 expression

Description	Orientation	DNA sequence 5'-3'
ABL1	FW	5'-TGGAGATAACACTCTAAGCATAACTAAAGGT-3'
	RV	5'-GATGTAGTTGCTTGGGACCCA-3'
	Probe	5'FAM-CCATTTTTGGTTTGGGCTTCACACCATT- TAMRA 3'
c.o.Rag2	FW	5'-TCTGAAACCGGGTATTGGAT- 3'
	RV	5'-GGCACCCATGTATTAATGTCC-3'
	Probe	Probe: 56 probe library Roche, FAM NFQ
PTBP2	FW	5'-TCTCCATTCCCTATGTTCATGC-3'

	RV	5'-GTTCCCGCAGAATGGTGAGGTG-3'
	Probe	[JOE]-ATGTTCCTCGGACCAACTTG-[BHQ1]
WPRE	FW	5'- GAGGAGTTGTGGCCCGTTGT-3'
	RV	5'-TGACAGGTGGTGGCAATGCC-3'
	Probe	[6FAM]-CTGTGTTTGCTGACGCAAC-[BHQ1]

Table S2: Repertoire analysis (murine) primers

Description	Orientation	DNA sequence
V gene segment-specific oligonucleotide		(5' -> 3', coding strand)
mVβ1	FW	CTGAATGCCCAGACAGCTCCAAGC
mVβ2	FW	TCACTGATACGGAGCTGAGGC
mVβ3.1	FW	CCTTGCAGCCTAGAAATTCAGT
mVβ4	FW	GCCTCAAGTCGCTTCCAACCTC
mVβ5.1	FW	CATTATGATAAAATGGAGAGAGAT
mVβ5.2	FW	AAGGTGGAGAGAGACAAAGGATTC
mVβ5.3 [#]	FW	AGAAAGGAAACCTGCCTGGTT
mVβ6	FW	CTCTCACTGTGACATCTGCCC
mVβ7	FW	TACAGGGTCTCACGGAAGAAGC
mVβ8.1	FW	CATTACTCATATGTCGCTGAC
mVβ8.2	FW	CATTATTCATATGGTGCTGGC
mVβ8.3	FW	TGCTGGCAACCTTCGAATAGGA
mVβ9	FW	TCTCTCTACATTGGCTCTGCAGGC
mVβ10	FW	ATCAAGTCTGTAGAGCCGGAGGA
mVβ11	FW	GCACTCAACTCTGAAGATCCAGAGC
mVβ12	FW	GATGGTGGGGCTTTCAAGGATC
mVβ13	FW	AGGCCTAAAGGAACTAACTCCCAC
mVβ14	FW	ACGACCAATTCATCCTAAGCAC
mVβ15	FW	CCCATCAGTCATCCCAACTTATCC
mVβ16	FW	CACTCTGAAAATCCAACCCAC
mVβ17#	FW	AGTGTTCCTCGAACTCACAG
mVβ18	FW	CAGCCGGCCAAACCTAACATTCTC
mVβ19 [#]	FW	CTGCTAAGAAACCATGTACCA
mVβ20	FW	TCTGCAGCCTGGGAATCAGAA
C gene segment specific oligonucleotide		(5' -> 3', non-coding strand)
muTCB1-FAM	RV	FAM-CTTGGGTGGAGTCACATTTCTC

REFERENCES

- 1. Stephan, J. L.; Vlekova, V.; Deist, F. L.; Blanche, S.; Donadieu, J.; Saint-Basile, G. D.; Durandy, A.; Griscelli, C.; Fischer, A., Severe combined immunodeficiency: A retrospective single-center study of clinical presentation and outcome in 117 patients. The Journal of Pediatrics 1993. 123 (4), 564-572.
- 2. Yee, A.; De Ravin, S. S.; Elliott, E.; Ziegler, J. B., Severe combined immunodeficiency: A national surveillance study. Pediatric Allergy and Immunology 2008, 19 (4), 298-302.
- 3. Dorsey, M. J.; Puck, J. M., Newborn Screening for Severe Combined Immunodeficiency in the United States: Lessons Learned. Immunology and Allergy Clinics of North America 2019, 39 (1), 1-11.
- 4. Fischer, A.; Hacein-Bey-Abina, S.; Cavazzana-Calvo, M., 20 years of gene therapy for SCID. Nature Immunology 2010. 11 (6), 457-460.
- 5. Bousfiha, A.; Jeddane, L.; Picard, C.; Ailal, F.; Bobby Gaspar, H.; Al-Herz, W.; Chatila, T.; Crow, Y. J.; Cunningham-Rundles, C.; Etzioni, A.; Franco, J. L.; Holland, S. M.; Klein, C.; Morio, T.; Ochs, H. D.; Oksenhendler, E.; Puck, J.; Tang, M. L. K.; Tangye, S. G.; Torgerson, T. R.; Casanova, J.-L.; Sullivan, K. E., The 2017 IUIS Phenotypic Classification for Primary Immunodeficiencies. Journal of Clinical Immunology 2018, 38 (1), 129-143.
- 6. Gaspar, H. B.; Qasim, W.; Davies, E. G.; Rao, K.; Amrolia, P. J.; Veys, P., How I treat severe combined immunodeficiency. Blood 2013, 122 (23), 3749-3758.
- 7. Schwarz, K.; Gauss, G. H.; Ludwig, L.; Pannicke, U.; Li, Z.; Lindner, D.; Friedrich, W.; Seger, R. A.; Hansen-Hagge, T. E.; Desiderio, S.; Lieber, M. R.; Bartram, C. R., RAG mutations in human B cell-negative SCID. Science 1996, 274 (5284), 97-9.
- 8. Grunebaum, E., Bone Marrow Transplantation for Severe Combined Immune Deficiency. JAMA 2006, 295 (5), 508.
- 9. Griffith, L. M.; Cowan, M. J.; Notarangelo, L. D.; Puck, J. M.; Buckley, R. H.; Candotti, F.; Conley, M. E.; Fleisher, T. A.; Gaspar, H. B.; Kohn, D. B.; Ochs, H. D.; O'Reilly, R. J.; Rizzo, J. D.; Roifman, C. M.; Small, T. N.; Shearer, W. T., Improving cellular therapy for primary immune deficiency diseases: Recognition, diagnosis, and management. Journal of Allerov and Clinical Immunology 2009, 124 (6), 1152-1160.e12.
- 10. Cavazzana-Calvo, M.; Fischer, A., Gene therapy for severe combined immunodeficiency: are we there yet? Journal of Clinical Investigation 2007, 117 (6), 1456-1465.
- 11. Gaspar, H. B.; Thrasher, A. J., Gene therapy for severe combined immunodeficiencies. 2005, 5 (9), 1175-1182.
- 12. Cowan, M. J.; Yu, J.; Facchino, J.; Chag, S.; Fraser-Browne, C.; Long-Boyle, J.; Kawahara, M.; Sanford, U.; Oh, J.; Teoh, S.; Punwani, D.; Dara, J.; Dvorak, C. C.; Broderick, L.; Hu, D.; Miller, H. K.; Petrovic, A.; Malech, H. L.; McIvor, R. S.; Puck, J., Early Outcome of a Phase I/II Clinical Trial (NCT03538899) of Gene-Corrected Autologous CD34+ Hematopoietic Cells and Low-Exposure Busulfan in Newly Diagnosed Patients with Artemis-Deficient Severe Combined Immunodeficiency (ART-SCID). Biology of Blood and Marrow Transplantation 2020, 26 (3), S88-S89.
- 13. Garcia-Perez, L.; van Eggermond, M.; van Roon, L.; Vloemans, S. A.; Cordes, M.; Schambach, A.; Rothe, M.; Berghuis, D.; Lagresle-Peyrou, C.; Cavazzana, M.; Zhang, F.; Thrasher, A. J.; Salvatori, D.; Meij, P.; Villa, A.; Van Dongen, J. J. M.; Zwaginga, J.-J.; van der Burg, M.; Gaspar, H. B.; Lankester, A.; Staal, F. J. T.; Pike-Overzet, K., Successful Preclinical Development of Gene Therapy for Recombinase-Activating Gene-1-Deficient SCID. Molecular Therapy Methods & Clinical Development 2020, 17, 666-682.
- 14. Yates, F.; Malassis-SéRis, M. L.; Stockholm, D.; Bouneaud, C. C.; Larousserie, F. D. R.; Noguiez-Hellin, P.; Danos, O.; Kohn, D. B.; Fischer, A.; De Villartay, J.-P.; Cavazzana-Calvo, M., Gene therapy of RAG-2-/- mice: sustained correction of the immunodeficiency. Blood 2002, 100 (12), 3942-3949.
- 15. Hacein-Bey-Abina, S.; Garrigue, A.; Wang, G. P.; Soulier, J.; Lim, A.; Morillon, E.; Clappier, E.; Caccavelli, L.; Delabesse, E.; Beldjord, K.; Asnafi, V.; Macintyre, E.; Dal Cortivo, L.; Radford, I.; Brousse, N.; Sigaux, F.; Moshous, D.; Hauer, J.; Borkhardt, A.; Belohradsky, B. H.; Wintergerst, U.; Velez, M. C.; Leiva, L.; Sorensen, R.; Wulffraat, N.; Blanche, S.; Bushman, F. D.; Fischer, A.; Cavazzana-Calvo, M., Insertional oncogenesis in 4 patients after retrovirus-mediated gene therapy of SCID-X1. Journal of Clinical Investigation 2008, 118 (9), 3132-3142.

- 16. Hacein-Bey-Abina, S., LMO2-Associated Clonal T Cell Proliferation in Two Patients after Gene Therapy for SCID-X1. Science 2003, 302 (5644), 415-419.
- 17. Howe, S. J.; Mansour, M. R.; Schwarzwaelder, K.; Bartholomae, C.; Hubank, M.; Kempski, H.; Brugman, M. H.; Pike-Overzet, K.; Chatters, S. J.; De Ridder, D.; Gilmour, K. C.; Adams, S.; Thornhill, S. I.; Parsley, K. L.; Staal, F. J. T.; Gale, R. E.; Linch, D. C.; Bayford, J.; Brown, L.; Quaye, M.; Kinnon, C.; Ancliff, P.; Webb, D. K.; Schmidt, M.; Von Kalle, C.; Gaspar, H. B.; Thrasher, A. J., Insertional mutagenesis combined with acquired somatic mutations causes leukemogenesis following gene therapy of SCID-X1 patients. Journal of Clinical Investigation 2008, 118 (9), 3143-3150.
- 18. Wu, C.; Dunbar, C. E., Stem cell gene therapy: the risks of insertional mutagenesis and approaches to minimize genotoxicity. Front Med 2011, 5 (4), 356-371.
- 19. Van Til, N. P.; De Boer, H.; Mashamba, N.; Wabik, A.; Huston, M.; Visser, T. P.; Fontana, E.; Poliani, P. L.; Cassani, B.; Zhang, F.; Thrasher, A. J.; Villa, A.; Wagemaker, G., Correction of Murine Rag2 Severe Combined Immunodeficiency by Lentiviral Gene Therapy Using a Codon-optimized RAG2 Therapeutic Transgene. Molecular Therapy 2012, 20 (10), 1968-1980.
- 20. Schambach, A.; Bohne, J.; Chandra, S.; Will, E.; Margison, G. P.; Williams, D. A.; Baum, C., Equal potency of gammaretroviral and lentiviral SIN vectors for expression of O6-methylguanine–DNA methyltransferase in hematopoietic cells. Molecular Therapy 2006, 13 (2), 391-400.
- 21. Halene, S.; Wang, L.; Cooper, R. M.; Bockstoce, D. C.; Robbins, P. B.; Kohn, D. B., Improved expression in hematopoietic and lymphoid cells in mice after transplantation of bone marrow transduced with a modified retroviral vector. Blood 1999, 94 (10), 3349-57.
- 22. Dull, T.; Zufferey, R.; Kelly, M.; Mandel, R. J.; Nguyen, M.; Trono, D.; Naldini, L., A Third-Generation Lentivirus Vector with a Conditional Packaging System. 1998, 72 (11), 8463-8471.
- 23. Knight, S.; Zhang, F.; Mueller-Kuller, U.; Bokhoven, M.; Gupta, A.; Broughton, T.; Sha, S.; Antoniou, M. N.; Brendel, C.; Grez, M.; Thrasher, A. J.; Collins, M.; Takeuchi, Y., Safer, Silencing-Resistant Lentiviral Vectors: Optimization of the Ubiquitous Chromatin-Opening Element through Elimination of Aberrant Splicing. Journal of Virology 2012, 86 (17), 9088-9095.
- 24. Pannetier, C.; Cochet, M.; Darche, S.; Casrouge, A.; Zöller, M.; Kourilsky, P., The sizes of the CDR3 hypervariable regions of the murine T-cell receptor beta chains vary as a function of the recombined germ-line segments. Proceedings of the National Academy of Sciences of the United States of America 1993, 90 (9), 4319-4323
- 25. Cordes, M.; Pike-Overzet, K.; Van Eggermond, M.; Vloemans, S.; Baert, M. R.; Garcia-Perez, L.; Staal, F. J. T.; Reinders, M. J. T.; Van Den Akker, E. B., ImSpectR: R package to quantify immune repertoire diversity in spectratype and repertoire sequencing data. Bioinformatics 2019.
- 26. Modlich, U.; Bohne, J.; Schmidt, M.; von Kalle, C.; Knöss, S.; Schambach, A.; Baum, C., Cell-culture assays reveal the importance of retroviral vector design for insertional genotoxicity. Blood 2006, 108 (8), 2545-2553.
- 27. Modlich, U.; Navarro, S.; Zychlinski, D.; Maetzig, T.; Knoess, S.; Brugman, M. H.; Schambach, A.; Charrier, S.; Galy, A.; Thrasher, A. J.; Bueren, J.; Baum, C., Insertional Transformation of Hematopoietic Cells by Self-inactivating Lentiviral and Gammaretroviral Vectors. Molecular Therapy 2009, 17 (11), 1919-1928.
- 28. Gabriel, R.; Kutschera, I.; Bartholomae, C. C.; von Kalle, C.; Schmidt, M., Linear amplification mediated PCR-localization of genetic elements and characterization of unknown flanking DNA. J Vis Exp 2014, (88), e51543.
- 29. Schmidt, M.; Hoffmann, G.; Wissler, M.; Lemke, N.; Müßig, A.; Glimm, H.; Williams, D. A.; Ragg, S.; Hesemann, C.-U.; Von Kalle, C., Detection and Direct Genomic Sequencing of Multiple Rare Unknown Flanking DNA in Highly Complex Samples. Human Gene Therapy 2001, 12 (7), 743-749.
- 30. Schmidt, M.; Schwarzwaelder, K.; Bartholomae, C.; Zaoui, K.; Ball, C.; Pilz, I.; Braun, S.; Glimm, H.; Von Kalle, C., High-resolution insertion-site analysis by linear amplification-mediated PCR (LAM-PCR). Nature Methods 2007, 4 (12), 1051-1057.
- 31. Gabriel, R.; Eckenberg, R.; Paruzynski, A.; Bartholomae, C. C.; Nowrouzi, A.; Arens, A.; Howe, S. J.; Recchia, A.; Cattoglio, C.; Wang, W.; Faber, K.; Schwarzwaelder, K.; Kirsten, R.; Deichmann, A.; Ball, C. R.; Balaggan, K. S.; Yáñez-Muñoz, R. J.; Ali, R. R.; Gaspar, H. B.; Biasco, L.; Aiuti, A.; Cesana, D.; Montini, E.; Naldini, L.; Cohen-Haguenauer, O.; Mavilio, F.; Thrasher, A. J.; Glimm, H.; Von Kalle, C.; Saurin, W.; Schmidt,

- M., Comprehensive genomic access to vector integration in clinical gene therapy. Nature Medicine 2009, 15 (12), 1431-1436.
- 32. Giordano, F. A.; Appelt, J. U.; Link, B.; Gerdes, S.; Lehrer, C.; Scholz, S.; Paruzynski, A.; Roeder, I.; Wenz, F.; Glimm, H.; von Kalle, C.; Grez, M.; Schmidt, M.; Laufs, S., High-throughput monitoring of integration site clonality in preclinical and clinical gene therapy studies. Mol Ther Methods Clin Dev 2015, 2, 14061.
- 33. Naldini, L.; Blomer, U.; Gallay, P.; Ory, D.; Mulligan, R.; Gage, F. H.; Verma, I. M.; Trono, D., In Vivo Gene Delivery and Stable Transduction of Nondividing Cells by a Lentiviral Vector. Science 1996, 272 (5259), 263-267.
- 34. Pike-Overzet, K.; Baum, C.; Bredius, R. G.; Cavazzana, M.; Driessen, G. J.; Fibbe, W. E.; Gaspar, H. B.; Hoeben, R. C.; Lagresle-Peyrou, C.; Lankester, A.; Meij, P.; Schambach, A.; Thrasher, A.; Van Dongen, J. J.; Zwaginga, J. J.; Staal, F. J., Successful RAG1-SCID gene therapy depends on the level of RAG1 expression. J Allergy Clin Immunol 2014, 134 (1), 242-3.
- 35. Dik, W. A.; Pike-Overzet, K.; Weerkamp, F.; De Ridder, D.; De Haas, E. F. E.; Baert, M. R. M.; Van Der Spek, P.; Koster, E. E. L.; Reinders, M. J. T.; Van Dongen, J. J. M.; Langerak, A. W.; Staal, F. J. T., New insights on human T cell development by quantitative T cell receptor gene rearrangement studies and gene expression profiling. Journal of Experimental Medicine 2005, 201 (11), 1715-1723.
- 36. Zheng, X.; Schwarz, K., Making V(D)J rearrangement visible: quantification of recombination efficiency in real time at the single cell level. J Immunol Methods 2006, 315 (1-2), 133-43.